Journal of Hepatocellular Carcinoma

Dovepress

open access to scientific and medical research

Open Access Full Text Article

ORIGINAL RESEARCH

# Disruption of Growth Hormone Receptor Signaling Abrogates Hepatocellular Carcinoma Development

Abedul Haque[1], Vishal Sahu[1], Jamie Lynne Lombardo[2], Lianchun Xiao[3], Bhawana George[1], Robert A Wolff[4], Jeffrey S Morris[3], Asif Rashid[2], John J Kopchick[5,6], Ahmed O Kaseb[4], Hesham M Amin[1,7]

[1]Department of Hematopathology, The University of Texas MD Anderson Cancer Center, Houston, TX, USA; [2]Department of Pathology, The University of Texas MD Anderson Cancer Center, Houston, TX, USA; [3]Department of Biostatistics, The University of Texas MD Anderson Cancer Center, Houston, TX, USA; [4]Department of Gastrointestinal Medical Oncology, The University of Texas MD Anderson Cancer Center, Houston, TX, USA; [5]Edison Biotechnology Institute, Heritage College of Osteopathic Medicine, Ohio University, Athens, OH, USA; [6]Department of Biomedical Sciences, Heritage College of Osteopathic Medicine, Ohio University, Athens, OH, USA; [7]MD Anderson Cancer Center UTHealth Graduate School of Biomedical Sciences, Houston, TX, USA

Correspondence: Hesham M Amin, Department of Hematopathology, Unit 072, Division of Pathology and Laboratory Medicine, The University of Texas MD Anderson Cancer Center, Houston, TX, 77030, USA, Tel +1 713 794-1769, Fax +1 713 792-7273, Email hamin@mdanderson.org; Ahmed O Kaseb, Department of Gastrointestinal Medical Oncology, The University of Texas MD Anderson Cancer Center, Houston, TX, 77030, USA, Tel +1 713 792-2828, Fax +1 713 745-1163, Email akaseb@mdanderson.org

**Introduction:** Hepatocellular carcinoma (HCC) is the most common type of primary liver cancers. It is an aggressive neoplasm with dismal outcome because most of the patients present with an advanced-stage disease, which precludes curative surgical options. Therefore, these patients require systemic therapies that typically induce small improvements in overall survival. Hence, it is crucial to identify new and promising therapeutic targets for HCC to improve the current outcome. The liver is a key organ in the signaling cascade triggered by the growth hormone receptor (GHR). Previous studies have shown that GHR signaling stimulates the proliferation and regeneration of liver cells and tissues; however, a definitive role of GHR signaling in HCC pathogenesis has not been identified.

**Methods:** In this study, we used a direct and specific approach to analyze the role of GHR in HCC development. This approach encompasses mice with global ($Ghr^{-/-}$) or liver-specific ($LiGhr^{-/-}$) disruption of GHR expression, and the injection of diethylnitrosamine (DEN) to develop HCC in these mice.

**Results:** Our data show that DEN induced HCC in a substantial majority of the $Ghr^{+/+}$ (93.5%) and $Ghr^{+/-}$ (87.1%) mice but not in the $Ghr^{-/-}$ (5.6%) mice ($P < 0.0001$). Although 57.7% of $LiGhr^{-/-}$ mice developed HCC after injection of DEN, these mice had significantly fewer tumors than $LiGhr^{+/+}$ ($P < 0.001$), which implies that the expression of GHR in the liver cells might increase tumor burden. Notably, the pathologic, histologic, and biochemical characteristics of DEN-induced HCC in mice resembled to a great extent human HCC, despite the fact that etiologically this model does not mimic this cancer in humans. Our data also show that the effects of DEN on mice livers were primarily related to its carcinogenic effects and ability to induce HCC, with minimal effects related to toxic effects.

**Conclusion:** Collectively, our data support an important role of GHR in HCC development, and suggest that exploiting GHR signaling may represent a promising approach to treat HCC.

**Keywords:** hepatocellular carcinoma, growth hormone receptor, *Ghr* knockout mouse, diethylnitrosamine

## Introduction

Hepatocellular carcinoma (HCC) is the dominant type of liver cancers, constituting ~75% of the total.[1] It is an aggressive neoplasm with a poor prognosis because ~80% of the patients are diagnosed at an advanced stage, which excludes curative treatment modalities such as surgical resection and liver transplantation.[2] Currently, advanced-stage HCC is treated with limited options for systemic therapies. For instance, sorafenib, a multi-kinase inhibitor, was approved for HCC treatment in 2008 based on Phase III SHARP trial that demonstrated a modest overall survival (OS) benefit as compared to placebo (10.7 vs 7.9 months, hazard ratio [HR] 0.69; $P < 0.001$).[3] Additional kinase inhibitors including lenvatinib, regorafenib, ramucirumab, and cabozantinib were approved in first or second-line settings with OS improvements of only 1.6 to 2.8 months vs placebo.[4–7] Immune checkpoint blockade was also assessed in HCC, and the anti-PD-1 antibodies nivolumab and pembrolizumab mostly failed as

Received: 31 March 2022
Accepted: 20 July 2022
Published: 15 August 2022

**Graphical Abstract**

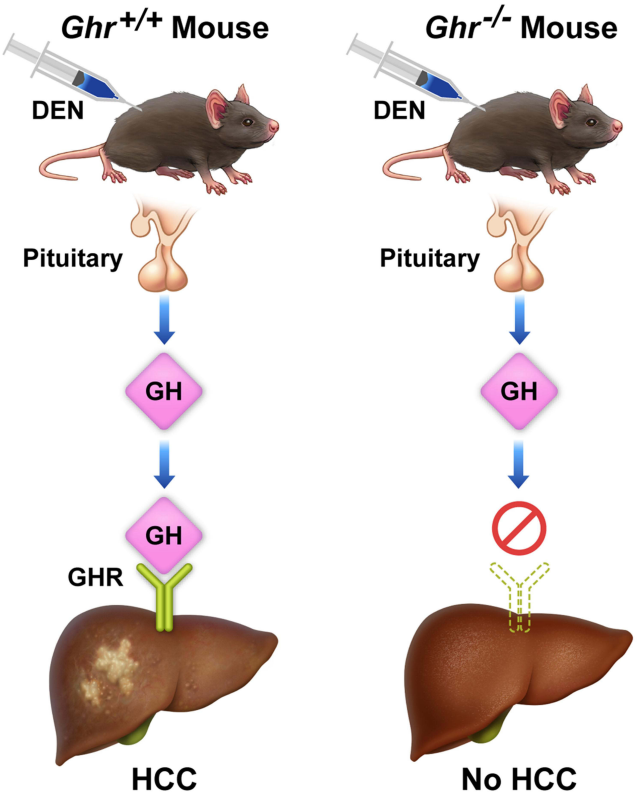


monotherapies.[8,9] More recently, the combination of atezolizumab (anti-PD-L1) plus bevacizumab (anti-VEGF-A) was approved as first-line therapy, based on phase III IMbrave150 trial that assessed this regimen vs sorafenib and yielded a progression-free survival (PFS) of only 6.8 vs 4.3 months, HR 0.59; $P < 0.001$, and objective response rate of 27% vs 12%.[10] However, it was soon discovered through preclinical and clinical investigations that immune checkpoint blockade, particularly as monotherapy, may not be effective in HCC patients with nonalcoholic steatohepatitis (NASH).[11–13]

The limited success of systemic therapies could be attributed, at least in part, to the diverse, complex, and poorly understood pathogenesis of HCC. For instance, the risk factors for HCC include chronic liver diseases such as NASH, liver cirrhosis, and hepatitis B and C viral infections. Other risk factors include excessive alcohol consumption, type 2 diabetes, obesity, metabolic syndrome, and ingestion of food contaminated with aflatoxin $B_1$.[14–17] Moreover, numerous pathways that involve growth factors, cell differentiation and development, nuclear signaling, and noncoding RNA are deregulated in HCC.[18] To add to its pathogenetic complexity, genetic aberrations such as amplifications of chromosomes 6p21 *(VEGFA)* and 11q13 *(FGF19/CNND1)*, deletions in chromosome 9 *(CDKN2A)*, and mutations in the *TERT, CTNNB1*, and *TP53* genes occur in HCC.[19,20] Therefore, effective systemic treatment of HCC remains a challenge, and it is critical to better our understanding of the pathogenesis of this cancer in order to develop new candidates that have legitimate therapeutic potential.

The growth hormone (GH) receptor (GHR) is the prototypical class I cytokine receptor.[21] GHR plays essential physiological roles related to regulating growth during childhood and adolescence, metabolism, and aging.[22] Signaling via GHR, which lacks kinase activity, is mediated through binding GH. This binding causes auto-phosphorylation of 2 GHR-associated JAK2 molecules, which subsequently activate transcription factors STAT3 and STAT5, and downstream molecules IRS-1, AKT, and ERK.[23] Nonetheless, GHR signaling can also be executed via JAK2-independent mechanisms.[24] An important outcome of GHR activation is stimulation of the production and secretion, mainly by the liver cell, of type I insulin-like growth factor (IGF-I).[25,26]

Through a negative feedback mechanism, IGF-I secreted by the liver inhibits the release of GH from somatotropic cells of the anterior pituitary.[27,28] Hence, the liver is considered a major target of GHR action.

In addition to its physiologic roles in the liver, previous studies implicated GHR signaling in HCC pathogenesis. Notably, these studies were performed in vitro or in vivo after stimulation of HCC cell lines by GH,[29–31] or in *Gh* transgenic mouse models.[32,33] In the current study, we tested the hypothesis that specific inhibition of GHR signaling abrogates HCC development. In contrast to the previous studies, we employed a direct strategy by testing the effects of specific inhibition of GHR signaling through targeted disruption of the *GHR* gene. Furthermore, we analyzed the effects of global vs liver-specific *GHR* gene disruption on HCC development and progression.

# Materials and Methods

## Reagents and Antibodies

Diethylnitrosamine (DEN), (catalogue number: N0258; MilliporeSigma, Burlington, MA) was dissolved in saline and stored at 4°C until used. Antibodies specific to pSTAT3$^{Tyr705}$ (9145), STAT3 (12640), pERK1/2$^{Thr202/Tyr204}$ (4370), ERK1/2 (4695), pGSK-3α/β$^{Ser21/9}$ (9331), GSK-3α/β (9315), p-c-Jun$^{Ser73}$ (3270), c-Jun (9165), pIGF-IR$^{Tyr1135/1136}$ (3024), IGF-IR (9750), Ki-67 (12202) (Cell Signaling, Cambridge, MA), BCL-2 (sc-7382), BCL-xL/xS (sc-1041) (Santa Cruz Biotechnology, Delaware, CA), and β-Actin (A2228), (MilliporeSigma) were used.

## Mice

GHR wild type (*Ghr*$^{+/+}$), GHR-heterozygous (*Ghr*$^{+/-}$), liver-specific GHR wild type (*LiGhr*$^{fl/fl}$ or *LiGhr*$^{+/+}$), and liver-specific GHR knockout (*LiGhr*$^{fl/fl}$:Alb Cre and *LiGhr*$^{-/-}$) mice were previously described.[34,35] Mice were maintained in a pathogen-free environment with controlled humidity and 12 h light/dark cycles.

## DEN-Induced HCC in Mice and Sample Collection

Mice experiments were performed in accordance with the National Institutes of Health's Guide for the Care and Use of Laboratory Animals and after approval of our Institutional Animal Care and Use Committee. To induce HCC, 2-week-old mice were injected with DEN (25 mg/kg) or saline (control) intraperitoneally and maintained for 36–40 weeks. HCC development was monitored every other week by visual observation and palpation to detect enlargement of the upper abdomen. After euthanasia, blood was collected by using cardiac puncture and left for 30 min at room temperature to clot. Serum was separated by centrifuging at 2000 rpm (376*g*) for 10 min in a pre-cooled Eppendorf centrifuge and stored at −80°C until analyzed. Body weight (before euthanasia), liver weight, and the number of tumors in the liver were recorded. Liver tissues were fixed in formalin and embedded in paraffin for histology. Portions of the livers were collected in RNA*later* stabilization solution for RNA isolation (AM7020; ThermoFisher, Waltham, MA) and snap frozen in liquid nitrogen for quantitative real time-PCR (qRT-PCR) and Western blotting (WB).

## Enzyme-Linked Immunosorbent Assay (ELISA)

Mouse-specific ELISA kits were used to measure circulating alpha-fetoprotein (AFP) (MAFP00; R&D Systems, St. Louis, MO), IGF-I (MG100; R&D Systems), and GH (EKU04609; Bio-Matik, Wilmington, DE). Briefly, serum samples were diluted according to the manufacturer's recommended protocols. Standards and samples were used simultaneously in each experimental setup. Optical densities were measured using a microplate reader (CLARIOstar; BMG Labtech, NC). Serum concentrations were calculated according to equations of linear standard curves generated by plotting optical densities and standard concentrations.

## Aspartate Aminotransferase (AST) and Alanine Aminotransferase (ALT) Measurement

Serum concentrations of AST (A7561-150) and ALT (A7526-150) were measured using kinetic assay-based kits (Pointe Scientific, Canton, MI). Briefly, 96-well plates were used where serum (10 µL) was pipetted in each well, and 100 µL of prewarmed (5 min at 37°C) working reagent was added to each well. Plates were subsequently incubated in a microplate

reader for 1 min at 37°C. Initial incubation absorbance was recorded every minute for 3 min. Mean absorbance difference/min and concentrations of AST and ALT were calculated according to the manufacturer's instructions.

## qRT-PCR

Total RNA was extracted from frozen liver tissues stored in RNA*later* stabilization solution (ThermoFisher) using RNeasy Mini Kit (Qiagen, Germantown, MD). RNA (1 µg) was reverse transcribed to cDNA using Super Script III cDNA Synthesis Kit (Invitrogen, Waltham, MA) according to the manufacturer's protocol. Quantitative real-time PCR (qPCR) was carried out by First SYBER Green Master Mix (Applied Biosystems, Waltham, MA). Briefly, cDNA (2 µL) and target specific forward and reverse primers were mixed with cyber green master mix in 96 well PCR plate. Mouse-specific primer (Integrated DNA Technologies, Coralville, IA) sequences for *Ghr* were as follows: forward 5′-TTTACCCCCAGTCCCAGTTC-3′; reverse 5′-TCAATGAACTCGACCCAGGA-3′, *Tnf*: forward 5′-GCCTCTTCTCATTCCTGCTT-3′; reverse 5′-CACTTGGTGGTTTG CTACGA-3′, *Il6*: forward 5′-TTCCATCCAGTTGCCTTCTT-3′; reverse 5′-ATTTCCACGATTTCCC AGAG-3′, *Il10*: forward 5′-GGACAACATACTGCTAACCGACTC-3′ and reverse 5′-AAAATCACTCTTCAC CTGCTCCAC-3′. PCR was performed using 7500 Fast Real-time PCR System (ThermoFisher). The optimized PCR conditions were 95°C (initial denaturation) for 5 min followed by 40 cycles at 95°C for 30 sec and 60°C for 60 sec. Gene expression levels were determined as the changes relative to the mean value of the reference gene (*Actb*).

## Western Blotting (WB)

Frozen liver tissues were homogenized using ice-cold radioimmunoprecipitation assay (RIPA) lysis buffer (9806; Cell Signaling). After sonication and centrifugation, the extracted proteins were recovered in the supernatant and mixed with sample buffer. Protein concentrations were determined using a protein assay kit (Bio-Rad, Hercules, CA). Equal protein amounts from each sample were separated on 10–12% sodium dodecyl sulfate–polyacrylamide gel, transferred to a polyvinylidene difluoride membrane (MilliporeSigma), and incubated with specific primary antibodies. Protein bands were detected with an enhanced chemiluminescence kit (Pierce Biotechnology, Waltham, MA). β-Actin was used as loading control.

## Immunohistochemical Staining (IHC)

Formalin-fixed and paraffin-embedded liver sections were deparaffinized using xylene and gradient alcohol concentration, washed, and subjected to antigen retrieval for 25 min in a steamer using 1× Target Retrieval Solution (S1699; Dako, Carpinteria, CA). Then, samples were placed for 20 min at room temperature, washed, and incubated for 30 min in 3% $H_2O_2$ to block endogenous peroxidase activity. Tissue sections were then washed in Protein Block Serum-Free solution (X0909; Dako) for 30 min at room temperature. Primary antibody (Ki-67) diluted in blocking buffer (1:400) was added for overnight incubation at 4°C. Next, the slides were washed and incubated with the secondary antibody (K4063; EnVision+ Dual Link System-HRP, Dako) for 30 min. Thereafter, the slides were washed and developed using Liquid DAB+ Substrate Chromogen System (K3468; Dako). Hematoxylin was used for counterstaining. The hematoxylin and eosin (H&E)- and IHC-stained tissue sections were independently evaluated by at least 2 pathologists (from HMA, AR, and JLL). Thereafter, consensus was achieved via joint meetings.

## Statistical Analysis

SAS (9.4; SAS Institute Inc., Cary, NC) and Prism 9 for macOS (9.2; GraphPad Software, San Diego, CA) software were used for statistical analysis. Statistical differences for continuous outcomes were measured by using ANOVA and the Tukey method for adjustment of multiple comparisons or Student's *t*-test where appropriate. Statistical differences for categorical outcomes were measured by using Chi-square test/Fisher's exact test. $P < 0.05$ was considered statistically significant.

# Results

## Genotypic and Phenotypic Features of Mice After Global and Liver-Specific Disruption of *Ghr* Gene

Before DEN injection, we extracted tail DNA and performed PCR for genotypic confirmation (Figure 1A and B). Figure 1C illustrates examples of adult $Ghr^{+/+}$, $Ghr^{+/-}$, and $Ghr^{-/-}$ mice where global *Ghr* disruption was associated with a remarkable

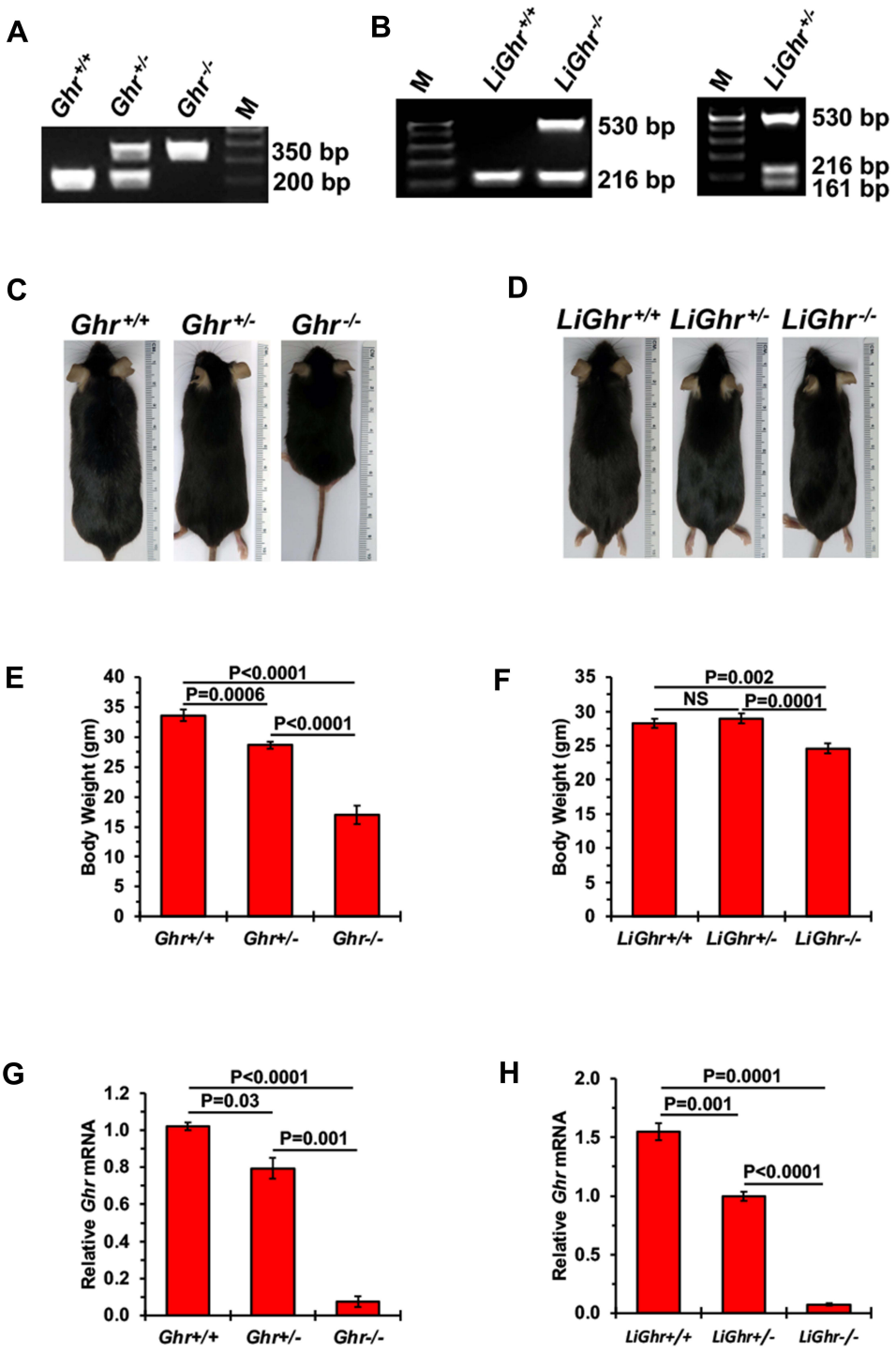


**Figure 1** Genotypic and phenotypic features of mice after global and liver-specific disruption of the *Ghr* gene. (**A**) Global (*Ghr*) and (**B**) liver-specific disruption of *Ghr* (*LiGhr*) was confirmed by genotyping using conventional polymerase chain reaction (PCR) from genomic DNA isolated from mice tails as described previously (smaller band denotes $Ghr^{+/+}$ mice while the larger band denotes $Ghr^{-/-}$ mice). Body sizes of representative mice examples from (**C**) the global $Ghr^{+/+}$, $Ghr^{+/-}$, and $Ghr^{-/-}$; and (**D**) the liver-specific $LiGhr^{+/+}$, $LiGhr^{+/-}$, and $LiGhr^{-/-}$ mice genotypes. Body weights of mice from the (**E**) global (n=31 in $Ghr^{+/+}$, n=31 in $Ghr^{+/-}$; n=18 in $Ghr^{-/-}$); and (**F**) $LiGhr^{+/+}$, $LiGhr^{+/-}$, and $LiGhr^{-/-}$ (n=25 in each group) genotype groups. (**G**) Levels of *Ghr* mRNA in the livers from global (n=3 in $Ghr^{+/+}$, n=2 in $Ghr^{+/-}$, n=3 in $Ghr^{-/-}$); and (**H**) liver-specific (n=2 in $LiGhr^{+/+}$, n=3 in $LiGhr^{+/-}$, n=3 in $LiGhr^{-/-}$) genotype groups. Results are shown as means ± SE.

reduction in body size. In contrast, this reduction was not observed when *Ghr* disruption was restricted to the liver (Figure 1D). Before euthanasia, $Ghr^{+/+}$ mice exhibited larger body weights than $Ghr^{+/-}$ and $Ghr^{-/-}$ mice ($P = 0.0006$ and $P < 0.0001$, respectively), and the weights of $Ghr^{+/-}$ mice were larger than the weights of $Ghr^{-/-}$ littermates ($P < 0.0001$) (Figure 1E).

Whereas significant differences were not observed between the weights of the $LiGhr^{+/+}$ and $LiGhr^{+/-}$ mice, the $LiGhr^{-/-}$ mice had smaller weights ($P < 0.01$ vs $LiGhr^{+/+}$ and $P = 0.0001$ vs $LiGhr^{+/-}$) (Figure 1F). The differences in body weights were gender-independent (Supplementary Figure 1). *Ghr* mRNA in the liver was measured by qRT-PCR. There was almost undetectable *Ghr* mRNA in $Ghr^{-/-}$ and $LiGhr^{-/-}$ mice compared with wild-type mice (Figure 1G and H). The heterozygous mice, $Ghr^{+/-}$ and $LiGhr^{+/-}$, demonstrated intermediate *Ghr* mRNA levels.

## *Ghr* Gene Disruption Inhibits HCC Development

Mice were injected with DEN (25 mg/kg) or saline (control) on postnatal day 14 and maintained for 36–40 weeks (Figure 2A). At necropsy, liver weights and tumor burden interpreted as the number of HCC tumors in the liver were determined. Tumors were not detected in any other organ. Representative examples of livers from DEN-treated $Ghr^{+/+}$, $Ghr^{+/-}$, and $Ghr^{-/-}$ mice and from a control $Ghr^{+/+}$ mouse not treated with DEN are shown in Figure 2B (upper row). Also, Figure 2B (lower row) shows examples of livers from $LiGhr^{+/+}$, $LiGhr^{+/-}$, and $LiGhr^{-/-}$ mice treated with DEN in addition to a representative control liver from $LiGhr^{+/+}$ littermate not treated with DEN. The $Ghr^{+/+}$ and $Ghr^{+/-}$ mice treated with DEN exhibited a significantly higher liver weight-to-body weight ratio than the $Ghr^{-/-}$ mice ($P < 0.001$; Figure 2C). All $Ghr^{-/-}$ mice were tumor-free except a female mouse who developed one tumor (1/18; 5.6%) (Figure 2D). In contrast, an overwhelming majority of $Ghr^{+/+}$ (29/31; 93.5%) and $Ghr^{+/-}$ (27/31; 87.1%) mice treated with DEN developed HCC ($P < 0.0001$). Of all mice that developed HCC, 50.9%, 47.4%, and 1.7% were of the $Ghr^{+/+}$, $Ghr^{+/-}$, and $Ghr^{-/-}$ genotypes, respectively (Figure 2E). Furthermore, the average number of HCC tumors in $Ghr^{+/+}$ and $Ghr^{+/-}$ mice was $13.7 \pm 2.9$ and $10.7 \pm 2.2$ tumors, respectively, vs $0.06 \pm 0.06$ tumors in $Ghr^{-/-}$ mice ($P < 0.001$; Figure 2F).

In addition, DEN-treated $LiGhr^{-/-}$ mice exhibited a significantly lower liver weight-to-body weight ratio than $LiGhr^{+/+}$ mice (Figure 2G; $P < 0.05$). In contrast to $Ghr^{-/-}$ mice (Figure 2D), HCC occurred more frequently in $LiGhr^{-/-}$ mice (Figure 2H). As depicted in Figure 2H, 20/26 (76.9%) of $LiGhr^{+/+}$ and $LiGhr^{+/-}$ mice and 15/26 (57.7%) of $LiGhr^{-/-}$ mice developed HCC. Significant differences were not detected among the *LiGhr* groups ($P = 0.21$). Of all mice with liver-specific genotype that developed HCC after DEN injection, 36.4%, 36.4%, and 27.2% belonged to the $LiGhr^{+/+}$, $LiGhr^{+/-}$, and $LiGhr^{-/-}$ groups, respectively (Figure 2I). Despite the high incidence of HCC in $LiGhr^{-/-}$ mice, the number of tumors in these mice was lower than $LiGhr^{+/+}$ and $LiGhr^{+/-}$ mice ($1.2 \pm 0.3$ tumors in $LiGhr^{-/-}$ mice vs $8.4 \pm 1.5$ and $4.5 \pm 1.1$ tumors in $LiGhr^{+/+}$ and $LiGhr^{+/-}$ groups, respectively) ($P < 0.001$ vs *LiGhr*; Figure 2J).

## DEN-Induced Liver Malignancy in $Ghr^{+/+}$ and $Ghr^{+/-}$ Mice Resembles Human HCC

Similar to the more pronounced HCC tumor burden in male compared to female patients, DEN induced a more pronounced tumor burden in male than female mice. Accordingly, male mice had significantly higher liver weight-to-body weight ratio and more tumors than female mice (Supplementary Figure 2). Importantly, DEN caused the development of HCC tumors that morphologically and histologically resembled to a great extent human HCC and that despite etiologically DEN-induced HCC does not mimic the human disease. Most of these tumors presented as relatively well-circumscribed nodules surrounded by benign liver tissues (2 examples of each of $Ghr^{+/+}$ and $Ghr^{+/-}$ tumors are shown in Figure 3A and B, respectively). Excluding the 1 female mouse mentioned above, all $Ghr^{-/-}$ mice treated with DEN did not develop HCC, and instead demonstrated normal liver architecture that was similar to the livers from control $Ghr^{+/+}$ mice not treated with DEN (Figure 3C and D). HCC tumors that developed in $LiGhr^{+/+}$, $LiGhr^{+/-}$, and $LiGhr^{-/-}$ mice showed similar histologic features (data not shown). IHC of Ki-67 was used to evaluate the proliferation index (PI), which was calculated as the number of positive cells per high-power field (HPF), with 10 HPF evaluated in each section (Figure 3E). HCC in $Ghr^{+/+}$ and $Ghr^{+/-}$ mice had significantly higher PI when compared with benign livers from DEN-treated $Ghr^{-/-}$ mice (Figure 3F; $Ghr^{+/+}$, $43.3 \pm 1.8$; $Ghr^{+/-}$, $31.3 \pm 2.4$; $Ghr^{-/-}$, $4.9 \pm 0.4$ Ki-67$^+$ cells/HPF; $P < 0.0001$). Also, HCC from $Ghr^{+/+}$ mice had a significantly higher PI than HCC from $Ghr^{+/-}$ mice ($P < 0.0001$). Whereas PI was significantly higher in HCC tumors from $Ghr^{+/+}$ and $Ghr^{+/-}$ mice than in normal liver tissues from wild-type mice not treated with DEN ($1.3 \pm 0.2$ Ki-67$^+$ cells/HPF; $P < 0.0001$), significant difference was not detected between PI in benign livers from $Ghr^{-/-}$ mice treated with DEN and normal liver tissues from wild-type mice not treated with DEN (wild-type mice data are not shown in Figure 3E and F).

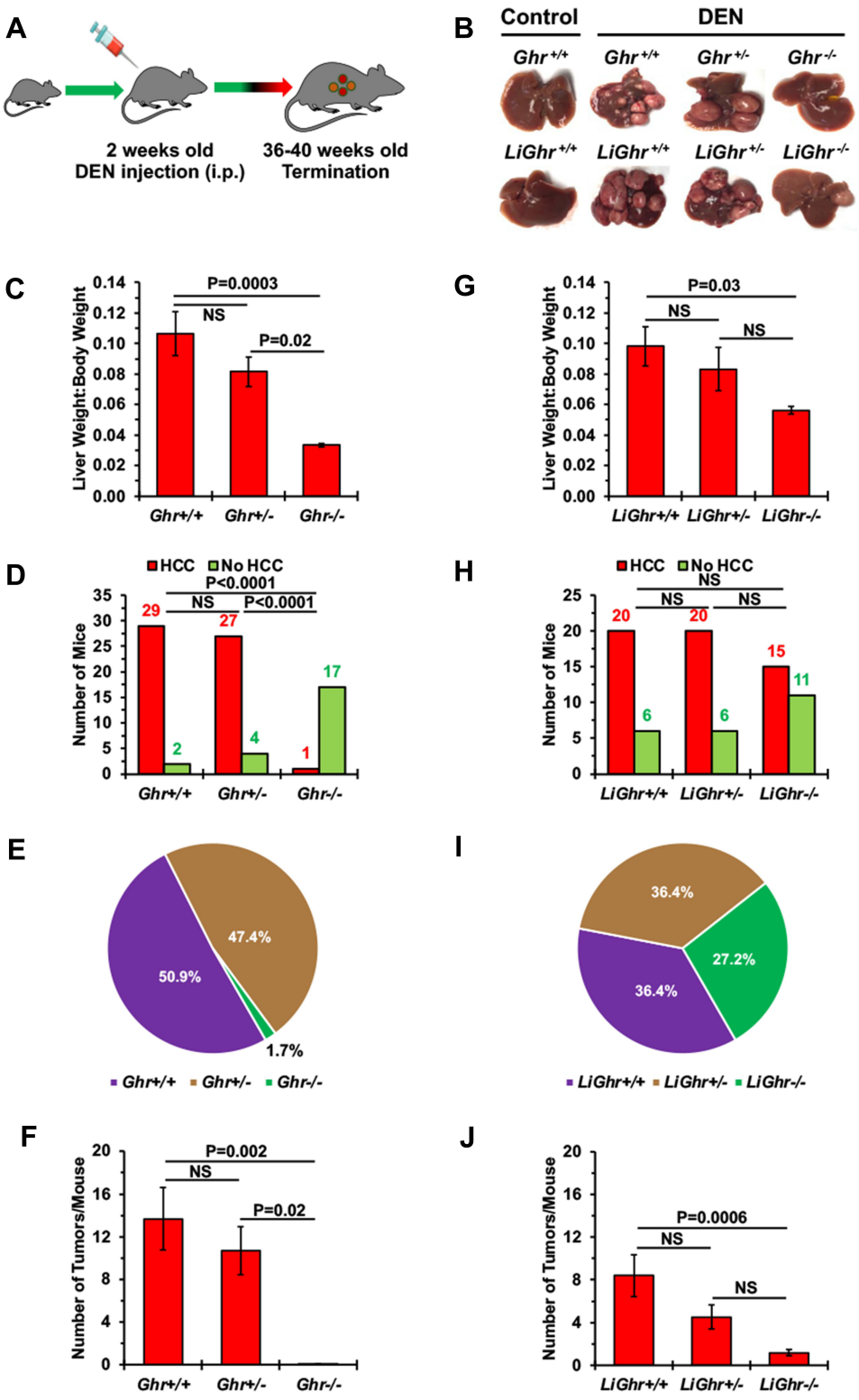


**Figure 2** Effects of the *Ghr* gene disruption on HCC development. (**A**) DEN-induced HCC mouse model. Mice were injected with DEN (25 mg/kg), or saline as control, on postnatal day 14 and maintained until they became 36–40 weeks old. (**B**) Representative examples of livers from global (upper row) and liver-specific genotypes mice (lower row) injected with DEN. Control $Ghr^{+/+}$ and $LiGhr^{+/+}$ mice were injected with saline only. For the *Ghr* global genotype, the liver weight-to-body weight ratios, number of mice with or without tumors, percentage of mice with HCC, and the number of tumors developed after DEN injection are shown in (**C**–**F**) respectively. For the *LiGhr* liver-specific genotype, the liver weight-to-body weight ratios, number of mice with or without tumors, percentage of mice with HCC, and the number of tumors developed after DEN injection are shown in (**G**–**J**) respectively. Results are shown as means ± SE in (**C, F, G**, and **I**), and as means in (**D** and **H**).


https://doi.org/10.2147/JHC.S368208 DovePress

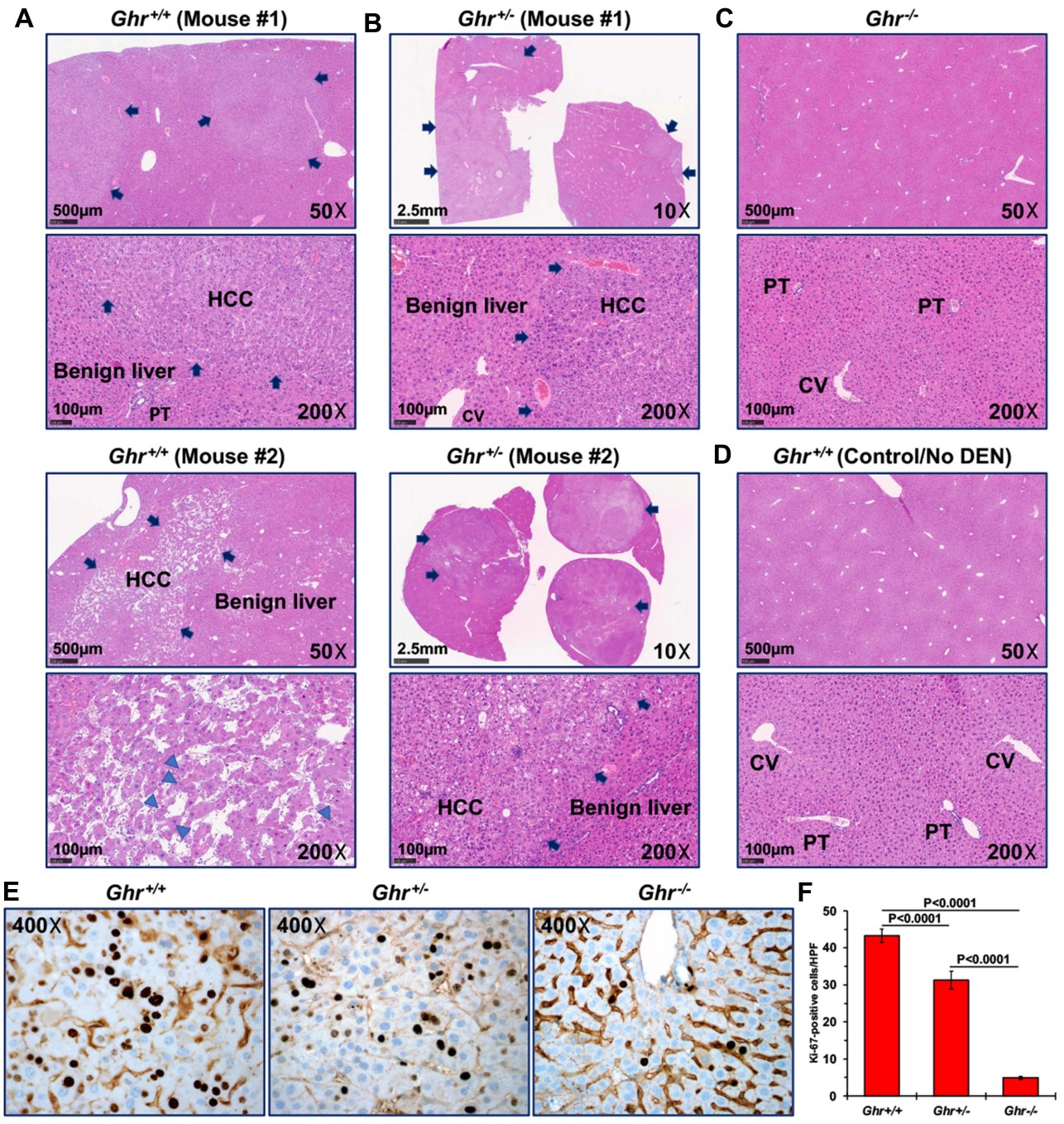


**Figure 3** DEN-induced HCC in *Ghr*$^{+/+}$ and *Ghr*$^{+/-}$ mice resembles to a great extent human HCC. Representative examples of hematoxylin and eosin-stained liver sections from (**A**, upper and lower panels) *Ghr*$^{+/+}$, (**B**, upper and lower panels) *Ghr*$^{+/-}$, and (**C**) *Ghr*$^{-/-}$ mice that were injected with DEN. (**D**) Liver sections from a control *Ghr*$^{+/+}$ mouse that was not injected with DEN is also shown as an example. Arrows highlight HCC tumor nodules in the *Ghr*$^{+/+}$ and *Ghr*$^{+/-}$ liver tissues. There are foci of markedly increased mitotic figures (arrowheads). HCC is not present in the livers from the *Ghr*$^{-/-}$ mouse treated with DEN and the *Ghr*$^{+/+}$ control mouse that was not treated with DEN. PT and CV denote portal tract and central vein, respectively. (**E**) IHC staining with Ki-67 shows increased PI in HCC that developed in *Ghr*$^{+/+}$ and *Ghr*$^{+/-}$ mice after DEN injection, compared with low PI in liver tissues from *Ghr*$^{-/-}$ mice that were also injected with DEN, yet did not develop HCC. (**F**) The means ± SE of the numbers of Ki-67$^{+}$ cells per HPF. The H&E photomicrographs were captured using the NanoZoomer S50 Digital slide scanner (Hamamatsu, Bridgewater, NJ), and the Ki-67 photomicrographs using an Olympus BX41 microscope (Olympus Scientific Solutions Americas Corp., Waltham, MA), Infinity 3 camera (Teledyne Lumenera, Ottawa, Ontario, Canada), and Infinity Capture software (version 6.3.2., Teledyne Lumenera). Original magnifications are shown.

Figure 4 illustrates selected protein changes in *Ghr*$^{+/+}$ livers harboring DEN-induced HCC vs normal livers from *Ghr*$^{-/-}$ mice treated with DEN. Findings in *Ghr*$^{+/+}$ and *Ghr*$^{-/-}$ mice not treated with DEN are shown as controls. HCC in *Ghr*$^{+/+}$ demonstrated findings that are mostly consistent with human HCC including increased expression of survival promoting

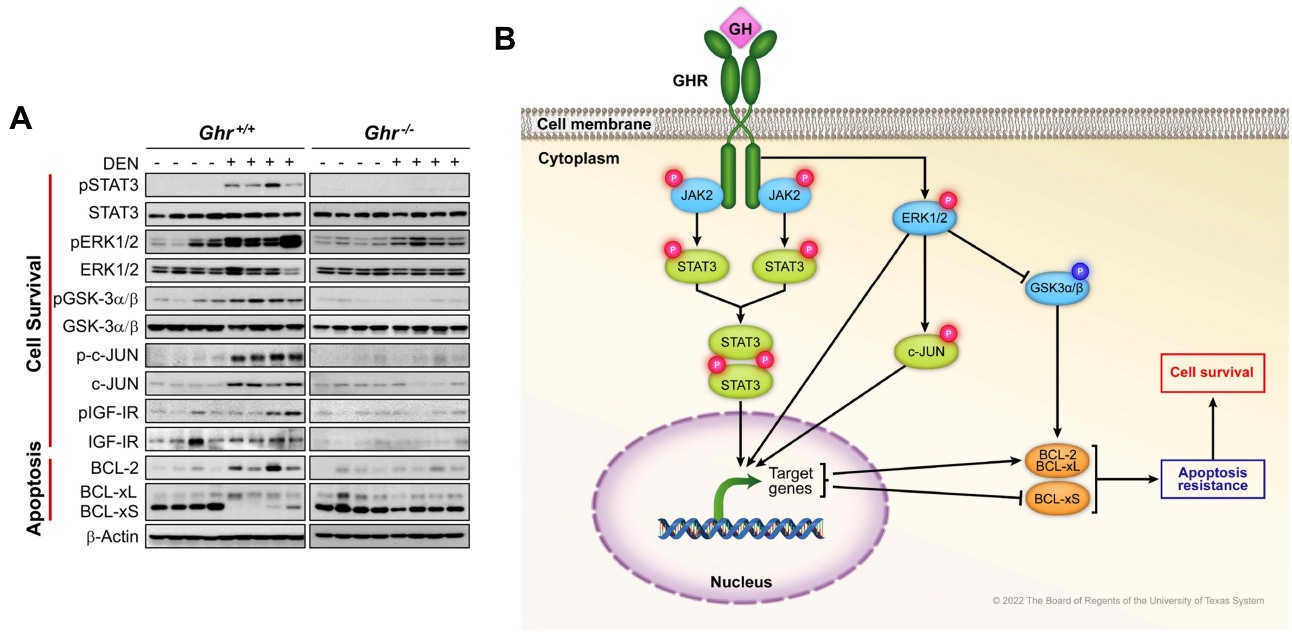


**Figure 4** Biochemical findings in *Ghr*$^{+/+}$ and Ghr$^{-/-}$ mice livers after DEN or without DEN injection. (**A**) WB analysis shows the expression of pSTAT3, pERK1/2, pGSK-3α/β, and p-c-JUN are upregulated in DEN-induced HCC tumors in *Ghr*$^{+/+}$ mice compared with normal liver tissues from control *Ghr*$^{+/+}$ mice not treated with DEN or from *Ghr*$^{-/-}$ mice treated or not treated with DEN. Some of the HCC tumors also show higher levels of pIGF-IR. Notably, there was a slight increase in pERK1/2, pGSK-3α/β, and pIGF-IR in some of the noncancerous livers from *Ghr*$^{+/+}$ mice not treated with DEN; nonetheless, these proteins revealed remarkably higher levels in DEN-induced HCC. Despite the lack of HCC development, the expression of pERK1/2 increased in *Ghr*$^{-/-}$ livers after treatment with DEN. It is possible that this increase resulted from toxic effects of DEN. However, the expression of pERK1/2 was much higher in HCC from *Ghr*$^{+/+}$ mice than in the livers from *Ghr*$^{-/-}$ mice when both groups were treated with DEN. Compared with control livers from *Ghr*$^{+/+}$ mice not treated with DEN, HCC tumors from *Ghr*$^{+/+}$ mice treated with DEN demonstrated upregulation of BCL-2 and BCL-xL, and downregulation of BCL-xS, which is consistent with apoptosis resistance. In contrast, expression of BCL-2 was downregulated and BCL-xS was upregulated in livers from the *Ghr*$^{-/-}$ mice that were treated or not treated with DEN. Furthermore, BCL-xL was mostly downregulated in the livers from these mice. (**B**) Hypothetical diagram, based on the WB results shown in (**A**), illustrating how GHR signaling promotes apoptosis resistance and cell survival in DEN-induced HCC (induces activation/upregulation:→; induces inhibition/downregulation:⊣; activation phosphorylation:●; inhibitory phosphorylation:●.

proteins pSTAT3, pERK1/2, pGSK-3α/β, and p-c-JUN. Some of these tumors also exhibited higher levels of pIGF-IR. Although there was a slight increase in pERK1/2, pGSK-3α/β, and pIGF-IR in some of the noncancerous livers from *Ghr*$^{+/+}$ mice not treated with DEN; these proteins revealed remarkably higher levels in DEN-induced HCC in *Ghr*$^{+/+}$ mice. Despite the lack of HCC development, the expression of pERK1/2 increased in *Ghr*$^{-/-}$ livers after treatment with DEN. It is possible that this increase resulted from toxic effects of DEN. Importantly, the expression of pERK1/2 was higher in DEN-induced HCC from *Ghr*$^{+/+}$ mice than in the livers from *Ghr*$^{-/-}$ mice after treatment with DEN. Compared with control livers from *Ghr*$^{+/+}$ littermates not treated with DEN, HCC tumors from *Ghr*$^{+/+}$ mice treated with DEN demonstrated findings consistent with resistance to apoptosis, ie, upregulation of BCL-2 and BCL-xL, and downregulation of BCL-xS. The expression of BCL-2 was downregulated, and BCL-xS was upregulated in livers from the *Ghr*$^{-/-}$ mice that were treated or not treated with DEN. Furthermore, BCL-xL was mostly downregulated in the livers from these mice.

## DEN Induces Minimal Toxic Effects on the Livers from *Ghr*$^{+/+}$ and *Ghr*$^{-/-}$ Mice

We also explored whether DEN causes nonspecific toxic effects on the liver that are not related to its carcinogenic effects and ability to induce HCC. Therefore, we analyzed several HCC-related parameters in *Ghr*$^{+/+}$ and *Ghr*$^{-/-}$ mice that were treated or not treated with DEN (Figure 5). The increase in liver weight-to-body weight ratio was observed in *Ghr*$^{+/+}$ mice with HCC tumors, and not in *Ghr*$^{+/+}$ mice not treated with DEN and *Ghr*$^{-/-}$ mice treated or not treated with DEN, which did not develop HCC (Figure 5A). Only the *Ghr*$^{+/+}$ mice with DEN-induced HCC tumors had significantly higher levels of circulating GH when compared with *Ghr*$^{+/+}$ mice not treated with DEN, which did not develop HCC (Figure 5B). Moreover, significantly higher levels of circulating GH were found in the *Ghr*$^{-/-}$ mice regardless of DEN status (Figure 5B). Only *Ghr*$^{+/+}$ mice, treated or not treated with DEN, demonstrated high levels of circulating IGF-I, whereas *Ghr*$^{-/-}$ mice, treated or not treated with DEN, had almost total lack of circulating IGF-I (Figure 5C). The

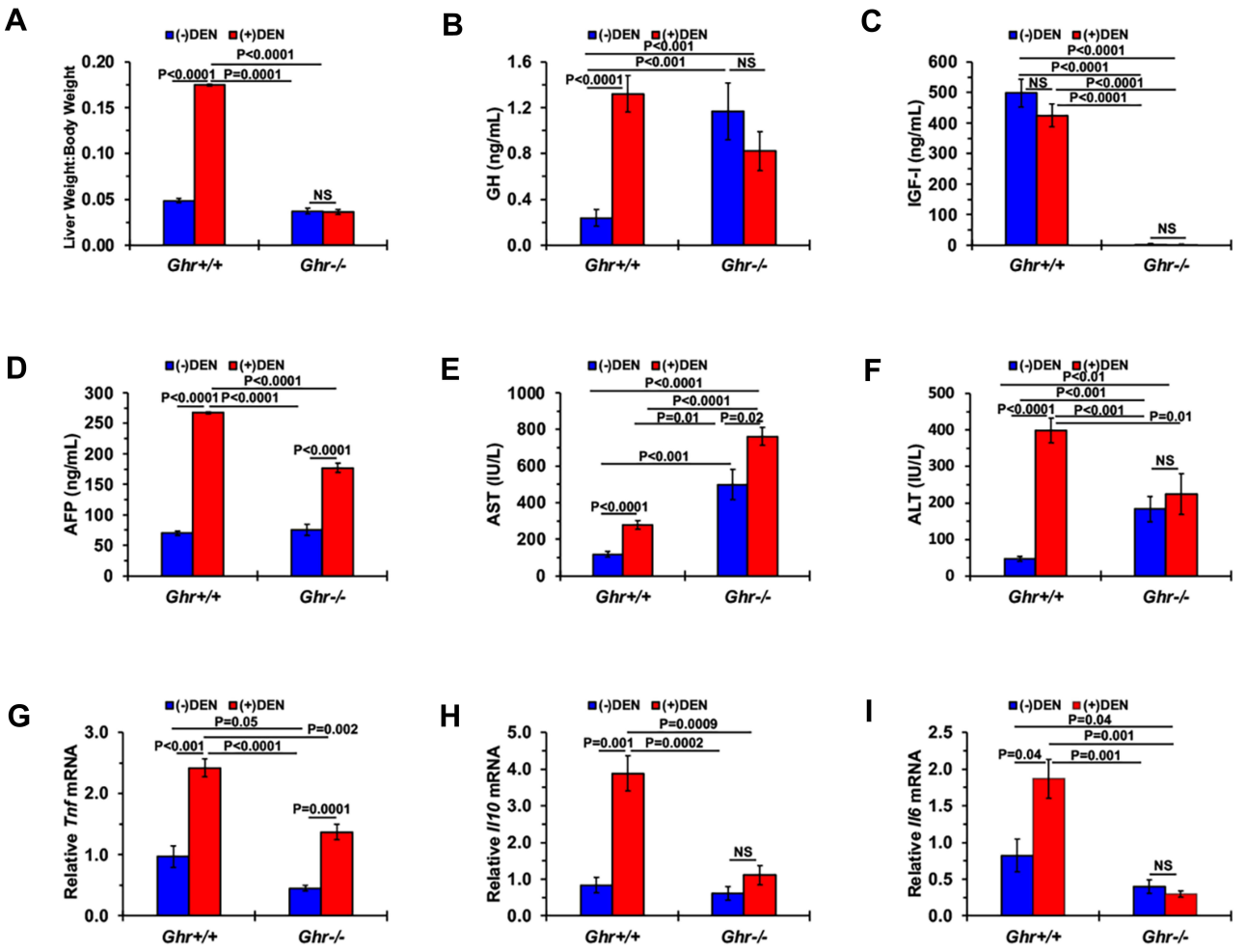


**Figure 5** Effects of DEN injection on the liver and circulating cytokines from $Ghr^{+/+}$ and $Ghr^{-/-}$ mice. (**A**) Liver weight-to-body weight ratios of 40-week-old $Ghr^{+/+}$ (n=8) and $Ghr^{-/-}$ (n=7) mice with or without DEN treatment. Serum levels of the following biomarkers are presented including (**B**) GH (n=5 in each group), (**C**) IGF-I (n=7 in each group), (**D**) AFP (n=5 in each group without DEN; n=6 in each group with DEN). (**E**) AST (n=9 in $Ghr^{+/+}$; n=7 in $Ghr^{-/-}$). (**F**) ALT (n=9 in $Ghr^{+/+}$; n=7 in $Ghr^{-/-}$). Relative mRNA levels of the following genes are shown including (**G**) *Tnf* (n=5 in each group), (**H**) *Il10* (n=4 in $Ghr^{+/+}$ without DEN; n=5 in other groups), (**I**) *Il-6* (n=3 in $Ghr^{+/+}$ without DEN; n=4 in other groups). Data are presented as means ± SE.

pronounced increase and decrease in circulating GH and IGF-I, respectively, have been previously reported in $Ghr^{-/-}$ mice,[34] and our data show that DEN had no effects on GH and IGF-I levels in these mice. Moreover, ALT, *Il10* mRNA, and *Il6* mRNA increased only in $Ghr^{+/+}$ mice who had DEN-induced HCC and not in $Ghr^{-/-}$ mice that were injected with DEN and did not develop HCC (Figure F, H and I). Our data also show that DEN had some effects that appear to be independent of HCC development. For instance, treatment with DEN increased AFP, AST, and *Tnf* mRNA (Figure 5D, E and G) in $Ghr^{-/-}$ mice that did not develop HCC. Collectively, our data support that the effects of DEN were primarily related to HCC development.

## Discussion

HCC is a devastating neoplasm with few approved systemic therapies that have a modest impact on improving outcome. Hence, it is critical to better our understanding of the mechanisms that underlie HCC pathogenesis in order to develop more effective systemic therapies. In the current study, we examined whether specific suppression of GHR signaling inhibits HCC development. To achieve our goals, we used a mouse model in which the *Ghr* gene is disrupted, either globally or only in the liver cells,[34–37] and utilized DEN to induce HCC in these mice. Our data show that DEN administration was associated with HCC development in the majority of the $Ghr^{+/+}$ and $Ghr^{+/-}$ mice but not in the $Ghr^{-/-}$ mice that have global disruption of *Ghr*. Although the frequency of DEN-induced HCC was higher in mice with liver-

specific than mice with global disruption of *Ghr* (*LiGhr*$^{-/-}$ vs *Ghr*$^{-/-}$), the *LiGhr*$^{-/-}$ mice had significantly fewer tumors than *LiGhr*$^{+/+}$ and *LiGhr*$^{+/-}$ mice, which suggests that the expression of GHR in liver cells might enhance HCC tumor burden. Our data also demonstrate that the pathologic, histologic, and biochemical features of DEN-induced HCC in mice resemble to a great extent those of HCC in humans. It is of important note that the HCC-related features were present despite the fact that etiologically DEN-induced HCC does not mimic human cancer.

The role of GHR signaling in cancer cell survival and proliferation has recently become the subject of increasing attention.[38] For instance, patients treated with GH are at higher risk of dying from cancer.[39] Moreover, patients with acromegaly, who have excessive production of GH and hyperactivation of GHR, suffer an increase in cancer incidence.[40–42] In contrast, individuals with *GHR* gene deficiency, eg, Laron syndrome patients, are protected from cancer and rarely die of it.[43,44]

Under the physiologic conditions, GHR signaling promotes the release of IGF-I from the liver, which in return suppresses the secretion of GH by the pituitary. Hence, the liver is considered a key organ in GHR signaling axis, and important roles of GHR in the pathogenesis of different types of liver diseases have been reported. For example, liver-specific disruption of *Ghr* in mice led to decreased IGF-I levels, insulin resistance, and development of hepatic steatosis.[45,46] Importantly, the association between GHR signaling and increased hepatic cell proliferation and HCC has been previously proposed. GHR was found to be highly expressed in human HCC tumors and increased GH levels in HCC patients correlated with worse outcomes.[47,48] In preclinical experiments, global disruption of the *Ghr* gene in mice was associated with impaired liver cell proliferation and tissue regeneration following partial hepatectomy.[49] The administration of GH upregulated the cell survival- and proliferation-promoting genes *Stat3* and *Mapk1* in livers from *Gh*-deficient dwarf rats.[50] Similarly, *Gh* transgenic mice suffer a remarkable increase in liver cell proliferation that leads to HCC, which has been attributed to activation of STAT3, ERK, AKT, EGFR, SRC, and mTOR.[32,51,52] Moreover, DEN-induced HCC occurred more frequently in *Gh* transgenic mice than in wild-type littermates.[33] Prior studies also demonstrated that GHR signaling stimulates the proliferation of HCC cells in vitro and the growth of HCC xenografts in nude mice.[29–31]

To our knowledge, the current study is the first to examine the impact of a direct and specific approach to inhibit GHR signaling, ie, disruption of the *Ghr* gene, on HCC development. DEN is a carcinogen that has been used to induce HCC in different laboratory animal species.[53–55] We have previously used DEN in miniature pigs, and found that the histopathological features of the developed HCC resemble to a great extent the human neoplasm.[56] Although etiologically DEN-induced HCC does not mimic this type of cancer in human patients, this model has several important pathological, histological, and biochemical similarities with human HCC. Similar to DEN-induced HCC in mice in our study, human HCC presents with comparable histopathological features, increased tumor burden in males than females, has higher proliferation index than normal liver tissue, and is associated with activation of STAT3, ERK1/2, GSK-3α/β, c-JUN, and IGF-IR.[18,57–59] Also, reminiscent to DEN-induced HCC, the human malignancy exhibits upregulation of BCL-xL and downregulation of BCL-xS, consistent with apoptosis resistance signature.[60,61] Whereas DEN-induced HCC in our study revealed upregulated BCL-2 expression, conflicting data related to this key antiapoptotic protein were reported in human HCC with some studies showing a total lack of expression and others demonstrating its expression only in a subset of human tumors.[62–64] The development of DEN-induced HCC was associated with increased circulating levels of GH, AFP, AST, and ALT, which are biomarkers that correlate with progression and response to therapy in HCC patients.[48,65] In addition, upregulation of the expression of *Il10, Il6*, and *Tnf* genes, which encode IL-10, IL-6, and TNF-α, respectively, was detected in the mice with DEN-induced HCC. These cytokines play key roles in HCC pathogenesis in humans.[66–68] Interestingly, AST levels were markedly elevated in *Ghr*$^{-/-}$ mice, with or without DEN administration, compared with *Ghr*$^{+/+}$ mice. Although the exact explanation of this finding is not known, it is possible that GHR plays a role in regulating the production and secretion of AST from the liver.

Our data are consistent with the previously reported genotypic and phenotypic characteristics of the mice with global and liver-specific *Ghr* gene disruption patterns.[34,35] Similar to the original reports, *Ghr*$^{-/-}$ mice, regardless of DEN administration, had increased levels of circulating GH and decreased levels of IGF-I than *Ghr*$^{+/+}$ mice. These findings can be attributed to the absence of GHR expression in liver cells, which leads to reduction of IGF-I release from the liver that produces 70–85% of serum IGF-I, and subsequent loss of its negative feedback effect on the secretion of GH from the pituitary.[34] Importantly, we also wanted to determine whether DEN causes toxic effects on the liver that are not related to its carcinogenic effects. In this regard, increases in only hepatic pERK1/2, circulating AFP and AST, and *Tnf*

mRNA were observed in *Ghr*$^{-/-}$ mice that did not develop HCC after DEN administration. Collectively, our data suggest that the effects of DEN on the mice livers were primarily related to its carcinogenic effects and HCC development. Despite the fact that some mice with the *LiGhr*$^{-/-}$ genotype developed HCC, these tumors were remarkably fewer than the tumors developed in mice with *Ghr* expression preserved in the liver, strongly suggesting that GHR expression in the liver may enhance HCC tumor burden. It is possible that the conserved expression of GHR in liver microenvironment bypassed its absence in the liver cells, which led to the development of HCC tumors in *LiGhr*$^{-/-}$ mice.

## Conclusions

In this study, we provide for the first time a direct evidence that the expression of GHR is required for HCC development. Our data suggest that exploiting GHR signaling might represent a novel therapeutic approach to treat HCC, which requires further systematic exploration in future studies.

## Abbreviations

AFP, alpha-fetoprotein; AKT, Ak strain transforming; ALT, alanine aminotransferase; AST, aspartate aminotransferase; ANOVA, analysis of variance; BCL-2, B-cell leukemia/lymphoma 2; BCL-xS/L, B-cell lymphoma-extra small/large, c-Jun, transcription factor Jun; DAB, 3,3'-diaminobenzidine; DEN, diethylnitrosamine; EGFR, epidermal growth factor receptor; DNA, deoxyribonucleic acid; ELISA, enzyme-linked immunosorbent assay; ERK, extracellular signal-regulated kinase; GH, growth hormone; GHR, growth hormone receptor; GSK, glycogen synthase kinase; H&E, hematoxylin and eosin; HCC, hepatocellular carcinoma; IGF-I, type I insulin-like growth factor; IGF-IR, type I insulin-like growth factor receptor; IHC, immunohistochemistry; IL, interleukin; IRS-1, insulin receptor substrate 1; JAK2, Janus kinase 2; Ki-67, marker of proliferation Ki-67; LiGhr; liver-specific growth hormone receptor; OS, overall survival; KO, knockout; LiGhr, liver-specific growth hormone receptor; mTOR, mammalian target of rapamycin; PD-1, programmed death protein 1; PD-L1, programmed death-ligand 1; PFS, progression-free survival; qRT-PCR, quantitative real-time reverse transcription polymerase chain reaction; RIPA, radioimmunoprecipitation assay; RNA, ribonucleic acid; SRC, SRC proto oncogene, non-receptor tyrosine kinase; STAT, signal transducer and activator of transcription; Tnf; tumor necrosis factor; WB, Western blotting.

## Ethical Standards

The mice experiments were performed in accordance with the National Institutes of Health's Guide for the Care and Use of Laboratory Animals and after approval by MD Anderson Cancer Center Animal Care and Use Committee.

## Acknowledgments

We thank Mr. Jordan Pietz for outstanding assistance with the generation of Figure 4B and the Graphical Abstract.

## Author Contributions

Authors made a significant contribution to the work reported, whether that is in the conception, study design, execution, acquisition of data, analysis and interpretation; took part in drafting, revising or critically reviewing the article; gave final approval of the version to be published; have agreed on the journal to which the article has been submitted; and agree to be accountable for all aspects of the work.

## Funding

This work was supported in part by the National Institutes of Health/National Cancer Institute grants R01CA151533 (HMA) and R01CA260872 (AOK, HMA) and by an MD Anderson Cancer Center Bridge Funding Grant (HMA).

## Disclosure

Prof. Dr. Robert A Wolff reports royalties as co-editor of MD Anderson Manual of Medical Oncology from McGraw Hill, outside the submitted work. The authors declare no competing financial/non-financial interests related to this work.

## References


1. Petrick JL, Florio AA, Znaor A, et al. International trends in hepatocellular carcinoma incidence, 1978–2012.. *Int J Cancer*. 2020;147(2):317–330. doi:10.1002/ijc.32723
2. Huitzil-Melendez FD, Capanu M, O'Reilly EM, et al. Advanced hepatocellular carcinoma: which staging systems best predict prognosis? *J Clin Oncol*. 2010;28(17):2889–2895. doi:10.1200/JCO.2009.25.9895
3. Llovet JM, Ricci S, Mazzaferro V, et al. Sorafenib in advanced hepatocellular carcinoma. *N Engl J Med*. 2008;359(4):378–390. doi:10.1056/NEJMoa0708857
4. Zhu AX, Park JO, Ryoo BY, et al. Ramucirumab versus placebo as second-line treatment in patients with advanced hepatocellular carcinoma following first-line therapy with sorafenib (REACH): a randomised, double-blind, multicentre, Phase 3 trial. *Lancet Oncol*. 2015;16(7):859–870. doi:10.1016/S1470-2045(15)00050-9
5. Bruix J, Qin S, Merle P, et al. Regorafenib for patients with hepatocellular carcinoma who progressed on sorafenib treatment (RESORCE): a randomised, double-blind, placebo-controlled, phase 3 trial. *Lancet*. 2017;389(10064):56–66. doi:10.1016/S0140-6736(16)32453-9
6. Abou-Alfa GK, Meyer T, Cheng AL, et al. Cabozantinib in patients with advanced and progressing hepatocellular carcinoma. *N Engl J Med*. 2018;379(1):54–63. doi:10.1056/NEJMoa1717002
7. Kudo M, Finn RS, Qin S, et al. Lenvatinib versus sorafenib in first-line treatment of patients with unresectable hepatocellular carcinoma: a randomised phase 3 non-inferiority trial. *Lancet*. 2018;391(10126):1163–1173. doi:10.1016/S0140-6736(18)30207-1
8. El-Khoueiry AB, Sangro B, Yau T, et al. Nivolumab in patients with advanced hepatocellular carcinoma (CheckMate 040): an open-label, non-comparative, Phase 1/2 dose escalation and expansion trial. *Lancet*. 2017;389(10088):2492–2502. doi:10.1016/S0140-6736(17)31046-2
9. Finn RS, Ryoo BY, Merle P, et al. Pembrolizumab as second-line therapy in patients with advanced hepatocellular carcinoma in KEYNOTE-240: a randomized, double-blind, phase III trial. *J Clin Oncol*. 2020;38(3):193–202. doi:10.1200/JCO.19.01307
10. Finn RS, Qin S, Ikeda M, et al. Atezolizumab plus bevacizumab in unresectable hepatocellular carcinoma. *N Engl J Med*. 2020;382(20):1894–1905. doi:10.1056/NEJMoa1915745
11. Dudek M, Pfister D, Donakonda S, et al. Auto-aggressive $CXCR6^{+}$ T cells cause liver immune pathology in NASH. *Nature*. 2021;592(7854):444–449. doi:10.1038/s41586-021-03233-8
12. Pfister D, Núñez NG, Pinyol R, et al. NASH limits anti-tumor surveillance in immunotherapy-treated HCC. *Nature*. 2021;592(7854):450–456. doi:10.1038/s41586-021-03362-0
13. Hindson J. T cells in NASH and liver cancer: pathology and immunotherapy. *Nat Rev Gastroenterol Hepatol*. 2021;18(6):367. doi:10.1038/s41575-021-00461-1
14. McGlynn KA, Petrick JL, El-Serag H. Epidemiology of hepatocellular carcinoma. *Hepatology*. 2021;73 Suppl 1(Suppl1):4–13. doi:10.1002/hep.31288
15. Younossi Z, Stepanova M, Ong JP, et al. Nonalcoholic steatohepatitis is the fastest growing cause of hepatocellular carcinoma in liver transplant candidates. *Clin Gastroenterol Hepatol*. 2019;17(4):748–755.e3. doi:10.1016/j.cgh.2018.05.057
16. Simon TG, King LY, Chong DQ, et al. Diabetes, metabolic comorbidities, and risk of hepatocellular carcinoma: results from two prospective cohort studies. *Hepatology*. 2018;67(5):1797–1806. doi:10.1002/hep.29660
17. Liu Y, Chang CC, Marsh GM, Wu F. Population attributable risk of aflatoxin-related liver cancer: systemic review and meta-analysis. *Eur J Cancer*. 2012;48(14):2125–2136. doi:10.1016/j.ejca.2012.02.009
18. Garcia-Lezana T, Lopez-Canovas JL, Villanueva A. Signaling pathways in hepatocellular carcinoma. *Adv Cancer Res*. 2021;149:63–101. doi:10.1016/bs.acr.2020.10.002
19. Zucman-Rossi J, Villanueva A, Nault JC, Llovet JM. Genetic landscape and biomarkers of hepatocellular carcinoma. *Gastroenterology*. 2015;149(5):1226–1239.e4. doi:10.1053/j.gastro.2015.05.061
20. Schulze K, Nault JC, Villanueva A. Genetic profiling of hepatocellular carcinoma using next-generation sequencing. *J Hepatol*. 2016;65(5):1031–1042. doi:10.1016/j.jhep.2016.05.035
21. de Vos AM, Ultsch M, Kossiakoff AA. Human growth hormone and extracellular domain of its receptor: crystal structure of the complex. *Science*. 1992;255(5042):306–312. doi:10.1126/science.1549776
22. Dehkhoda F, Lee CMM, Medina J, Brooks AJ. The growth hormone receptor: mechanism of receptor activation, cell signaling, and physiological aspects. *Front Endocrinol*. 2018;9:35. doi:10.3389/fendo.2018.00035
23. Brooks AJ, Dai W, O'Mara ML, et al. Mechanism of activation of protein kinase JAK2 by the growth hormone receptor. *Science*. 2014;344(6185):1249783. doi:10.1126/science.1249783
24. Barclay JL, Kerr LM, Arthur L, et al. *In vivo* targeting of the growth hormone receptor (GHR) Box1 sequence demonstrates that the GHR does not signal exclusively through JAK2. *Mol Endocrinol*. 2010;24(1):204–217. doi:10.1210/me.2009-0233
25. Schwander JC, Hauri C, Zapf J, Froesch ER. Synthesis and secretion of insulin-like growth factor and its binding protein by the perfused rat liver: dependence on growth hormone status. *Endocrinology*. 1983;113(1):297–305. doi:10.1210/endo-113-1-297
26. Bick T, Amit T, Barkey RJ, Hertz P, Youdim MB, Hochberg Z. The interrelationship of growth hormone (GH), liver membrane GH receptor, serum GH-binding protein activity, and insulin-like growth factor I in the male rat. *Endocrinology*. 1990;126(4):1914–1920. doi:10.1210/endo-126-4-1914
27. Blum WF, Albertsson-Wikland K, Rosberg S, Ranke MB. Serum levels of insulin-like growth factor I (IGF-I) and IGF binding protein 3 reflect spontaneous growth hormone secretion. *J Clin Endocrinol Metab*. 1993;76(6):1610–1616. doi:10.1210/jcem.76.6.7684744
28. Junnila RK, List EO, Berryman DE, Murrey JW, Kopchick JJ. The GH/IGF-1 axis in ageing and longevity. *Nat Rev Endocrinol*. 2013;9(6):366–376. doi:10.1038/nrendo.2013.67
29. Li S, Hou G, Wang Y, Su X, Xue L. Influence of recombinant human growth hormone (rhGH) on proliferation of hepatocellular carcinoma cells with positive and negative growth hormone receptors in vitro. *Tumori*. 2010;96(2):282–288.
30. Kong X, Wu W, Yuan Y, et al. Human growth hormone and human prolactin function as autocrine/paracrine promoters of progression of hepatocellular carcinoma. *Oncotarget*. 2016;7(20):29465–29479. doi:10.18632/oncotarget.8781
31. Chen YJ, You ML, Chong QY, et al. Autocrine human growth hormone promotes invasive and cancer stem cell-like behavior of hepatocellular carcinoma cells by STAT3 dependent inhibition of CLAUDIN-1 expression. *Int J Mol Sci*. 2017;18(6):1274. doi:10.3390/ijms18061274

32. Snibson KJ, Bhathal PS, Hardy CL, Brandon MR, Adams TE. High, persistent hepatocellular proliferation and apoptosis precede hepatocarcinogenesis in growth hormone transgenic mice. *Liver*. 1999;19(3):242–252. doi:10.1111/j.1478-3231.1999.tb00042.x
33. Snibson KJ, Bhathal PS, Adams TE. Overexpressed growth hormone (GH) synergistically promotes carcinogen-initiated liver tumor growth by promoting cellular proliferation in emerging hepatocellular neoplasms in female and male GH-transgenic mice. *Liver*. 2001;21(2):149–158. doi:10.1034/j.1600-0676.2001.021002149.x
34. Zhou Y, Xu BC, Maheshwari HG, et al. A mammalian model for Laron syndrome produced by targeted disruption of the mouse growth hormone receptor/binding protein gene (the Laron mouse). *Proc Natl Acad Sci U S A*. 1997;94(24):13215–13220. doi:10.1073/pnas.94.24.13215
35. List EO, Berryman DE, Funk K, et al. Liver-specific GH receptor gene-disrupted (LiGHRKO) mice have decreased endocrine IGF-I, increased local IGF-I, and altered body size, body composition, and adipokine profile. *Endocrinology*. 2014;155(5):1793–1805. doi:10.1210/en.2013-2086
36. Wang Z, Prins GS, Coschigano KT, et al. Disruption of growth hormone signaling retards early stages of prostate carcinogenesis in the C3(1)/T antigen mouse. *Endocrinology*. 2005;146(12):5188–5196. doi:10.1210/en.2005-0607
37. Zhang X, Mehta RG, Lantvit DD, et al. Inhibition of estrogen-independent mammary carcinogenesis by disruption of growth hormone signaling. *Carcinogenesis*. 2007;28(1):143–150. doi:10.1093/carcin/bgl138
38. Clayton PE, Banerjee I, Murray PG, Renehan AG. Growth hormone, the insulin-like growth factor axis, insulin and cancer risk. *Nat Rev Endocrinol*. 2011;7(1):11–24. doi:10.1038/nrendo.2010.171
39. Swerdlow AJ, Higgins CD, Adlard P, Preece MA. Risk of cancer in patients treated with human pituitary growth hormone in the UK, 1959–1985: a cohort study. *Lancet*. 2002;360(9329):273–277. doi:10.1016/s0140-6736(02)09519-3
40. Cheung NW, Boyages SC. Increased incidence of neoplasia in females with acromegaly. *Clin Endocrinol*. 1997;47(3):323–327. doi:10.1046/j.1365-2265.1997.2561053.x
41. Popovic V, Damjanovic S, Micic D, et al. Increased incidence of neoplasia in patients with pituitary adenomas. *Clin Endocrinol*. 1998;49(4):441–445. doi:10.1046/j.1365-2265.1998.00536.x
42. Kauppinen-Mäkelin R, Sane T, Välimäki MJ, et al. Increased cancer incidence in acromegaly – a nationwide survey. *Clin Endocrinol*. 2010;72(2):278–279. doi:10.1111/j.1365-2265.2009.03619.x
43. Guevara-Aguirre J, Balasubramanian P, Guevara-Aguirre M, et al. Growth hormone receptor deficiency is associated with a major reduction in pro-aging signaling, cancer, and diabetes in humans. *Sci Transl Med*. 2011;3(70):70ra13. doi:10.1126/scitranslmed.3001845
44. Werner H, Lapkina-Gendler L, Achlaug L, et al. Genome-wide profiling of Laron syndrome patients identifies novel cancer protection pathways. *Cells*. 2019;8(6):596. doi:10.3390/cells8060596
45. Fan Y, Menon RK, Cohen P, et al. Liver specific deletion of growth hormone receptor reveals essential role of growth hormone signaling in hepatic lipid metabolism. *J Biol Chem*. 2009;284(30):19937–19944. doi:10.1074/jbc.M109.014308
46. Liu Z, Cordoba-Chacon J, Kineman RD, et al. Growth hormone control of hepatic lipid metabolism. *Diabetes*. 2016;65(12):3598–3609. doi:10.2337/db16-0649
47. García-Caballero T, Mertani HM, Lambert A, et al. Increased expression of growth hormone and prolactin receptors in hepatocellular carcinomas. *Endocrine*. 2000;12(3):265–271. doi:10.1385/ENDO:12:3:
48. Morris JS, Hassan MM, Zohner YE, et al. Hepatoscore-14: measures of biological heterogeneity significantly improve prediction of hepatocellular carcinoma risk. *Hepatology*. 2021;73(6):2278–2292. doi:10.1002/hep.31555
49. Zerrad-Saadi A, Lambert-Blot M, Mitchell C, et al. GH receptor plays a major role in liver regeneration through the control of EGFR and ERK1/2 activation. *Endocrinology*. 2011;152(7):2731–2741. doi:10.1210/en.2010-1193
50. Thompson BJ, Shang CA, Waters MJ. Identification of genes induced by growth hormone in rat liver using cDNA arrays. *Endocrinology*. 2000;141(11):4321–4324. doi:10.1210/endo.141.11.7874
51. Iida K, Del Rincon JP, Kim DS, et al. Tissue-specific regulation of growth hormone (GH) receptor and insulin-like growth factor-I gene expression in the pituitary and liver of GH-deficient (lit/lit) mice and transgenic mice that overexpress bovine GH (bGH) or a bGH antagonist. *Endocrinology*. 2004;145(4):1564–1570. doi:10.1210/en.2003-1486
52. Miquet JG, González L, Matos MN, et al. Transgenic mice overexpressing GH exhibit hepatic upregulation of GH-signaling mediators involved in cell proliferation. *J Endocrinol*. 2008;198(2):317–330. doi:10.1677/JOE-08-0002
53. Lapis K, Zalatnai A, Timár F, Thorgeirsson UP. Quantitative evaluation of lysozyme- and CD68-positive Kupffer cells in diethylnitrosamine-induced hepatocellular carcinoma in monkeys. *Carcinogenesis*. 1995;16(12):3083–3085. doi:10.1093/carcin/16.12.3083
54. Castro-Gil MP, Sánchez-Rodríguez R, Torres-Mena JE, et al. Enrichment of progenitor cells by 2-acetylaminofluorene accelerates liver carcinogenesis induced by diethylnitrosamine in vivo. *Mol Carcinog*. 2021;60(6):377–390. doi:10.1002/mc.23298
55. Kurhe Y, Caputo M, Cansby E, et al. Antagonizing STK25 signaling suppresses the development of hepatocellular carcinoma through targeting metabolic, inflammatory, and pro-oncogenic pathways. *Cell Mol Gastroenterol Hepatol*. 2022;13(2):405–423. doi:10.1016/j.jcmgh.2021.09.018
56. Mitchell J, Tinkey PT, Avritscher R, et al. Validation of a preclinical model of diethylnitrosamine-induced hepatic neoplasia in Yucatan miniature pigs. *Oncology*. 2016;91(2):90–100. doi:10.1159/000446074
57. Ladenheim MR, Kim NG, Nguyen P, et al. Sex differences in disease presentation, treatment and clinical outcome of patients with hepatocellular carcinoma: a single-center cohort study. *BMJ Open Gastroenterol*. 2016;3(1):e000107. doi:10.1136/bmjgast-2016-000107
58. Eferl R, Ricci R, Kenner L, et al. Liver tumor development: c-Jun antagonizes the proapoptotic activity of p53. *Cell*. 2003;112(2):181–192. doi:10.1016/s0092-8674(03)00042-4
59. Schmitz KJ, Wohlschlaeger J, Lang H, et al. Activation of the ERK and AKT signalling pathway predicts poor prognosis in hepatocellular carcinoma and ERK activation in cancer tissue is associated with hepatitis C virus infection. *J Hepatol*. 2008;48(1):83–90. doi:10.1016/j.jhep.2007.08.018
60. Takehara T, Liu X, Fujimoto J, Friedman SL, Takahashi H. Expression and role of Bcl-xL in human hepatocellular carcinoma. *Hepatology*. 2001;34(1):55–61. doi:10.1053/jhep.2001.25387
61. Beerheide W, Tan YJ, Teng E, Ting AE, Jedpiyawongse A, Srivatanakul P. Downregulation of proapoptotic proteins Bax and Bcl-Xs in p53 overexpressing hepatocellular carcinoma. *Biochem Biophys Res Commun*. 2000;273(1):54–61. doi:10.1006/bbrc.2000.2891
62. Zhao M, Zhang NX, Economou M, Blaha I, Laissue JA, Zimmermann A. Immunohistochemical detection of bcl-2 protein in liver lesions: bcl-2 protein is expressed in hepatocellular carcinomas but not in liver cell dysplasia. *Histopathology*. 1994;25(3):237–245. doi:10.1111/j.1365-2559.1994.tb01323.x

63. Soini Y, Virkajärvi N, Lehto VP, Pääkkö P. Hepatocellular carcinomas with a high proliferation index and a low degree of apoptosis and necrosis are associated with a shortened survival. *Br J Cancer*. 1996;73(9):1025–1030. doi:10.1038/bjc.1996.199
64. Ravazoula P, Tsamandas AC, Kardamakis D, et al. The potential role of bcl-2 mRNA and protein expression in hepatocellular carcinomas. *Anticancer Res*. 2002;22(3):1799–1805.
65. Wen CP, Lin J, Yang YC, et al. Hepatocellular carcinoma risk prediction model for the general population: the predictive power of transaminases. *J Natl Cancer Inst*. 2012;104(20):1599–1611. doi:10.1093/jnci/djs372
66. He G, Dhar D, Nakagawa H, et al. Identification of liver cancer progenitors whose malignant progression depends on autocrine IL-6 signaling. *Cell*. 2013;155(2):384–396. doi:10.1016/j.cell.2013.09.031
67. Han Y, Chen Z, Yang Y, et al. Human $CD14^{+}$ $CTLA\text{-}4^{+}$ regulatory dendritic cells suppress T-cell response by cytotoxic T-lymphocyte antigen-4-dependent IL-10 and indoleamine-2,3-dioxygenase production in hepatocellular carcinoma. *Hepatology*. 2014;59(2):567–579. doi:10.1002/hep.26694
68. Tan W, Luo X, Li W, et al. TNF-α is a potential therapeutic target to overcome sorafenib resistance in hepatocellular carcinoma. *EBioMedicine*. 2019;40:446–456. doi:10.1016/j.ebiom.2018.12.047